

Effectiveness analysis of ship formation air defence based on deep belief network

eISSN 2051-3305

Received on 14th October 2019

Accepted on 19th November 2019

E-First on 9th July 2020

doi: 10.1049/joe.2019.1201

www.ietdl.org

Bo Li^{1,2} ✉, Haoran Luo¹, Yuanxun Wang¹, Daqing Chen³¹School of Electronics and Information, Northwestern Polytechnical University, Shanxi Xi'an, People's Republic of China²CETC Key Laboratory of Data Link Technology, Shanxi Xi'an, People's Republic of China³School of Engineering, London South Bank University, London, UK

✉ E-mail: libo803@nwpu.edu.cn

Abstract: Aiming at the problem of strong subjectivity and insufficient data utilisation in the traditional ship formation combat effectiveness analysis method, this study proposes a performance analysis fitting model based on deep belief network (DBN), which effectively reconstructs the combat model and improves the accuracy of the effectiveness analysis of the combat system. Firstly, the ship formation air defence effectiveness analysis index system is constructed, and then the structure and training method of the performance analysis fitting model are introduced. Finally, based on the formation of air defence combat, the performance analysis fitting model based on DBN and its comparative experiments are simulated and analysed. Simulation results verify the applicability and effectiveness of the model and method.

1 Introduction

As countries shift the focus of military development to the ocean, ship formations, as an important combat force in modern naval warfare, are receiving more and more attention from all countries [1]. The operational effectiveness of surface warship formations is a measure of warship formations' various tasks, and the analysis of its effectiveness is a hot issue.

On the one hand, the operational effectiveness analysis of surface warship formations is a complex problem that requires comprehensive consideration of integrated qualitative and quantitative information, as well as subjective and objective information [2]. The analysis of its effectiveness is not only to examine the operational effectiveness values that can be achieved based on current combat equipment, but also to be able to assess which factors have an impact on the operational effectiveness and how much impact it has; On the other hand, ship formation air defence operations have complex properties such as non-linear, multi-dimensional, non-monotonic, and will generate a large number of high-dimensional combat data in actual combat exercises or operational simulations. However, in a lot of practical work, it is found that the application of these data is still at a simple statistical level and is not fully utilised [3]. Therefore, how to use data to evaluate the effectiveness of combat systems is a very valuable issue.

The traditional combat system effectiveness evaluation mainly adopts methods based on experts, intuition, knowledge and logic, such as analytic hierarchy process (AHP) method [4], cloud model [5], etc. These methods are subjective in the evaluation process, resulting in great uncertainty and it is difficult to obtain effective results stably.

In view of the above problems, this paper introduces the relevant knowledge of deep learning into the ship formation air defence combat system. A performance evaluation fitting model based on deep belief network (DBN) is constructed by using deep learning's superior feature learning ability. The model is able to learn the appropriate and effective features from a large number of complex operational data, and then reconstruct the operational model. It solves the problem that the traditional method is insufficient for the utilisation of combat data and the subjectivity of the evaluation process is strong.

2 Formation air defence effectiveness evaluation index system

The construction of the performance analysis index system is the prerequisite for the performance analysis of the warship formation combat system. The system performance indicators of the warship formation air defence combat system can be obtained from the combination of subsystem performance indicators of the system, and the performance indicators of these subsystems are closely related to the equipment performance indicators. The meanings of the ship formation performance indicators, subsystem performance indicators, and equipment performance indicators are described below.

Equipment performance indicators are inherent characteristics of the physical components of the system equipment, which essentially reflect the capabilities of the system. This paper mainly refers to the equipment performance indicators of information detection system, command and control system and weapon strike system, such as missile quantity, kill radius, radar detection accuracy, radar detection range, information processing speed, information processing accuracy and so on. The sub-system performance indicator refers to the measure of the degree to which the different subsystems of the ship formation complete the relevant subtasks. It mainly includes the formation probability of the ship formation, the timeliness of the command, and the probability of damage to the target. The system performance indicator is a measure of the overall operational mission of the ship formation. There are different ways to choose depending on the angle of assessment. It mainly includes the interception probability of the incoming target, the probability of missile penetration, and so on.

From the above analysis, it can be seen that the equipment performance index, subsystem operational efficiency index and system operational efficiency index of the warship formation air defence combat system are numerous, and the complete construction and analysis work is extremely large. This paper mainly uses the system to verify the performance analysis fitting model. Therefore, the interception probability of the incoming target is selected as the system operational performance index from the interception angle of the incoming target. Analysis of its relationship with performance indicators is shown in Fig. 1.

Then the input of the system can be obtained through the design of the experimental scheme, and the output data is obtained

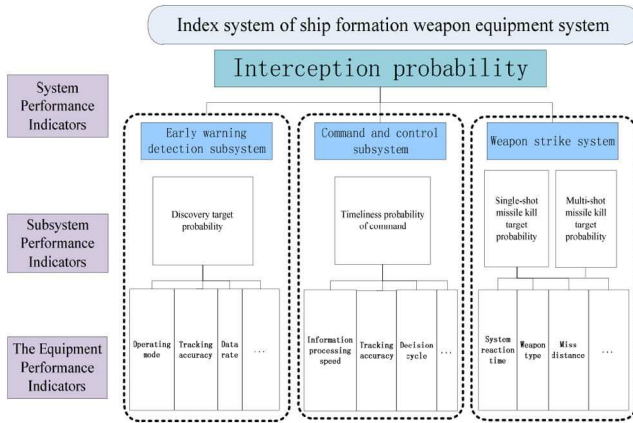


Fig. 1 Equipment performance indicators and system performance indicators related to intercept probability

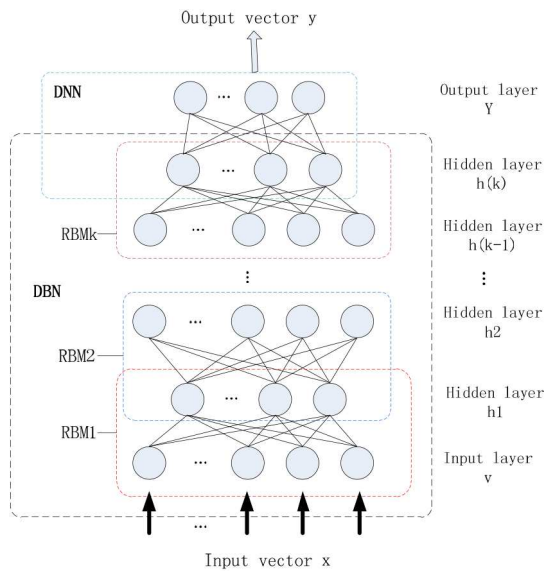


Fig. 2 DBN-based performance analysis fitting model

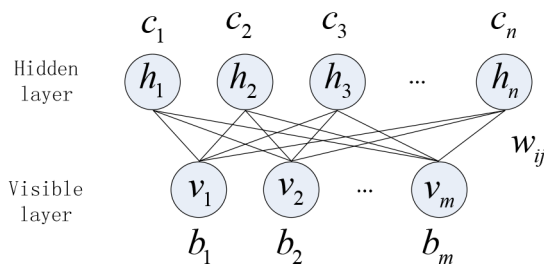


Fig. 3 Network structure of a restricted Boltzmann machine

through the simulation system. The performance of the system can be analysed using the obtained input and output data.

3 Performance analysis fitting model based on DBN

Standard-restricted Boltzmann machine is commonly used for the first layer of restricted Boltzmann machine (RBM), and also known as Bernoulli–Bernoulli restricted Boltzmann machine (BRBM). However, all of its nerve units can only take 0 or 1, which affects its application. Although some methods can be used to model a continuous distribution with a standard constrained Boltzmann machine, it is generally not sufficient to construct a good model for complex real data [6].

In order to extract the characteristics of real-valued data better, this paper will change the first layer (input layer) of the restricted Boltzmann machine that constitutes the DBN network from BRBM to Gauss–Bernoulli restricted Boltzmann machine (GRBM). The

Boltzmann machine is changed from BRBM to GRBM (Gaussian RBM, GRBM) [7], the remaining layers are still composed of BRBM.

Based on the excellent ability of DBN in extracting data features, a performance fitting analysis model is constructed [8]. Next, the structure and training methods of the performance analysis fitting model are mainly analysed.

3.1 Structure of the performance analysis fitting model

The performance analysis fitting model based on the DBN consists of a fully connected neural network and a DBN structure consisting of several layers of RBMs. The performance analysis fit model structure is shown in Fig. 2.

The hidden layer of the last layer of the restricted Boltzmann machine that forms the DBN and the fully connected back propagation (BP) neural network constitute the deep neural network (DNN), which serves as the regression layer for the entire performance analysis fitting network. The output feature vector of the last layer of the hidden layer of DBN is used as the input vector of the neural network. The pre-training process of DBN can be regarded as the process of parameter initialisation of the whole neural network. The output of the model is mainly the value of the system performance indicator, and the input data is the value of each key performance indicator that affects the final system performance indicator value. Each of the influencing factors can be divided again to form an input vector x , which forms a training sample with the output vector y .

3.2 Pre-training and tuning of performance analysis fitting models

DBN [9] is composed of multiple RBMs. The hidden layer of the first layer RBM is used as the display layer of the second RBM. After layer-by-layer superposition, a DBN structure is formed. The RBM training method can be applied to the DBN layer by layer training. The specific training process is as follows: firstly, the layer-by-layer unsupervised pre-training is performed by the restricted Boltzmann machine according to the layer-by-layer greedy method, and then the back-propagation algorithm is used for tuning. The network structure of the RBM is shown in Fig. 3.

It consists of a visible layer v and an implicit layer h . An RBM is an energy-based model that defines its energy function as

$$E(v, h, \theta) = - \sum_i v_i b_i - \sum_j h_j c_j - \sum_{i,j} v_i h_j w_{ij} \quad (1)$$

where $v = (v_i)$, $h = (h_j)$ represent the vector of the visible layer and the corresponding unit of the hidden layer, respectively; $\theta = \{W, b, c\}$ represents the set of all connection weights and parameters of the RBM; w_{ij} represents the symmetric connection weight between the visible layer and the corresponding unit of the hidden layer; b_i , c_j are the offset of the visible unit v_i and the hidden unit v_i , respectively.

Based on the energy function, the joint probability distribution of the visible and hidden layers is

$$p(v, h) = \frac{1}{Z} e^{-E(v, h)} \quad (2)$$

where Z is the normalisation coefficient, which makes the sum of all probability distributions equal to 1, which can be expressed as

$$Z = \sum_{v, h} e^{-E(v, h)}.$$

The probability when the visual unit $h_j = 1$ is

$$p(h_j = 1 | v) = \sigma \left(\sum_{i=1}^m w_{ji} v_i + c_j \right) \quad (3)$$

where $\sigma(x)$ represents a sigmoid activation function whose expression is related to the selected function.

The probability when the implicit unit $v_i = 1$ is

$$p(v_i = 1|h) = \sigma\left(\sum_{j=1}^n w_{ji}h_j + b_i\right) \quad (4)$$

For the RBM model introduced above, the training process is mainly to find a probability distribution that can generate training samples with maximum probability, that is, to find a weight vector \mathbf{W} that satisfies the requirements. In 2002, Hinton *et al.* [10] proposed the contrast divergence (CD) algorithm for the rapid training of RBM networks. It obtains the optimal value of the parameter by solving the negative gradient of the log-likelihood function. The process is shown in Fig. 4.

It should be noted that the visual layer structure constituting the DBN is different. The first layer of RBM that is commonly used to form a DBN is the standard-restricted Boltzmann machine, also known as the BRBM. However, because all its visible nodes and hidden nodes can only take 0 and 1 values, it is greatly limited in application. Although some methods can be used to model a continuous distribution with a standard constrained Boltzmann machine, it is generally not sufficient to construct a good model for complex real data [11].

In order to better extract the characteristics of real-valued data, this paper will replace the first-layer (visual layer) restricted Boltzmann machine that constitutes the DBN network from a standard RBM to a GRBM (Gaussian RBM, GRBM) [7], the remaining layers are still composed of standard RBM. The GRBM energy function is

$$E(\mathbf{v}, \mathbf{h}, \theta) = \frac{1}{2} \sum_i \frac{(v_i - b_i)^2}{\sigma^2} - \sum_{i,j} \frac{v_i h_j w_{ij}}{\sigma^2} - \sum_j h_j c_j \quad (5)$$

where σ^2 represents the variance of the input value of the visual node.

In the unsupervised pre-training phase, from the visible layer to the last hidden layer, each adjacent two layers of the DBN is treated as a restricted Boltzmann machine. First, the first RBM is trained using the CD algorithm to obtain the corresponding weight parameters. The RBM parameters are then fixed and used as input to continue training the next RBM of the construction until the end of the last restricted Boltzmann training.

Each layer of RBM constructed through the above process can only ensure that the weights in the layer are optimised for the feature extraction of the layer, and the error of the RBM of the previous layer is not corrected during the training process, and will gradually pass to the next layer. Therefore, in order to ensure the optimality of the overall result, it is necessary to further optimise the weight of the network.

The DBN is usually regarded as a DNN, and the parameters derived from the previous training are used as initial parameters of the entire network. Then use the backpropagation method to supervise the overall weight of this network. Specific steps are as follows:

(i) The minimum mean square error criterion is used to measure the update effect of the parameter. When the cost function is minimum, the parameter update is completed. The cost function is defined as follows:

$$E = \frac{1}{N} \sum_{i=1}^N (\hat{Y}_i(W^l, b^l) - Y_i)^2 \quad (6)$$

where E represents the mean squared error, \hat{Y}_i, Y_i represent the actual output and ideal output of the output layer, respectively, and W^l, b^l represents the weight and offset parameters of the l -layer to be learned.

(ii) The backpropagation algorithm is used to solve the gradient values of each layer of the network, and the weights and offset

Initialize connection weight \mathbf{W} and offset \mathbf{b}, \mathbf{c} ;

FOR One data in the training set \mathbf{X}

Give the value of \mathbf{X} to the visible unit $\mathbf{v}^{(0)}$ and calculate the probability that it makes the implicit unit $h_j^{(0)} = 1$:

$$p(h_j^{(0)} = 1 | \mathbf{v}^{(0)}) = \sigma(\mathbf{W}_j^T \mathbf{v}^{(0)});$$

Extract a sample from the calculated probability distribution: $h_j^{(0)} \sim P(h_j^{(0)} | \mathbf{v}^{(0)})$;

Use $h^{(0)}$ to reconstruct the visible layer $\mathbf{v}^{(1)}$ and calculate the probability that it makes the visible unit $v_i^{(1)} = 1$:

$$p(v_i^{(1)} = 1 | h^{(0)}) = \sigma(\mathbf{W}_i^T h^{(0)});$$

Extract samples from the visible layer: $\mathbf{v}^{(1)} \sim P(\mathbf{v}^{(1)} | h^{(0)})$;

Calculating the probability of the hidden layer unit $h_j^{(1)} = 1$ using the visible layer \mathbf{a} after reconstruction:

$$p(h_j^{(1)} = 1 | \mathbf{v}^{(1)}) = \sigma(\mathbf{W}_j^T \mathbf{v}^{(1)});$$

Update parameter: $\mathbf{w} \leftarrow \mathbf{w} + \epsilon_{CD} (P(h^{(0)} = 1 | \mathbf{v}^{(0)}) \mathbf{v}^{(0)r} - P(h^{(0)} = 1 | \mathbf{v}^{(1)}) \mathbf{v}^{(0)r})$, $\mathbf{b} = \mathbf{b} + \epsilon_{CD} (\mathbf{v}^{(0)} - \mathbf{v}^{(1)})$,

$$\mathbf{c} = \mathbf{c} + \epsilon_{CD} (P(h^{(0)} = 1 | \mathbf{v}^{(0)}) - P(h^{(1)} = 1 | \mathbf{v}^{(1)}))$$

UNTIL (Training set data cycle ends)

Output weight \mathbf{W} ;

Fig. 4 Comparison divergence algorithm calculation process

parameters of the network are updated by using the solved gradient values. The update process is as follows:

$$(\mathbf{W}^{(l)}, \mathbf{b}^{(l)}) \leftarrow \left\{ (\mathbf{W}^{(l)}, \mathbf{b}^{(l)}) - \epsilon \cdot \frac{\partial E}{\partial (\mathbf{W}^{(l)}, \mathbf{b}^{(l)})} \right\} \quad (7)$$

where ϵ represents the learning efficiency.

(iii) Through the above weight update rule, the weight is gradually adjusted to minimise the cost function value, thereby obtaining an optimal weight combination.

4 Simulation experiment

4.1 Simulation environment

The ship formation air defence effectiveness evaluation model of this paper is completed by using C++ programming language in VC++ 6.0 compilation environment. The performance analysis fitting model based on the DBN and the simulation analysis of the comparative experiment were completed using MATLAB 2015b.

The ship formation combat model considers the 16 performance indicators in Table 1 as input factors to the system, and the values of other factors are fixed. The output factor of the ship formation air defence combat model selects the intercept probability of the incoming target. The output factor value can be obtained by simulation after determining the input factors of the warship formation combat model. The value space and initial value of the system input factors are shown in Table 1.

4.2 Construction and analysis of the performance analysis fitting model

Next, we first focus on the number of layers of the network hidden layer and the number of neurons in each layer of the performance analysis fitting model, and analyse the influence of different structural parameters on the performance analysis fitting model.

4.2.1 Influence of model parameters and structure on performance fitting effect:

The system input indicators are randomly sampled, and 15,000 sets of experimental schemes are generated as the combat model input. The corresponding output factor values are obtained by using the warship formation combat model simulation. The 15,000 sets of data containing input factors and output factor values constitute experimental data. In the experiment, the evaluation index of the performance analysis fitting model is mainly selected from the perspective of error. The selected indicators are mainly the mean absolute percentage error:

$$\text{MAPE} = \frac{1}{N} \sum_{i=1}^N \left| \frac{y_{nh} - y_{sj}}{y_{sj}} \right| \quad (8)$$

and the root mean square error:

$$\text{RMSE} = \sqrt{\frac{1}{N} \sum_{i=1}^N |y_{nh} - y_s|^2} \quad (9)$$

The other parameters of the model are set as shown in Table 2.

In order to obtain the best model structure, first set the number of hidden cells in the first layer, and find the optimal number according to the evaluation index and fix it; Then add a hidden layer and determine the optimal number of hidden nodes in the new layer according to the above method; Add next hidden layers until the accuracy of the evaluation index is no longer improved.

Table 3 gives the evaluation index values for the model when selecting the number of different hidden layers and different nodes for each layer. There are three choices for hidden layers, which are 1, 2 and 3; there are six choices for each layer, which are 5, 10, 20, 30, 40, and 50. The data used is 16,000 sets of experimental data, which are divided into 14,000 sets of training data and 2000 sets of test data. These data are used to train the model and calculate the value of the evaluation index. In order to reduce the error caused by random sampling of the experimental samples, the model is trained 10 times according to the selected data amount, and then the values of the evaluation indexes are, respectively, calculated, and finally the average value is taken. The results are shown in Table 3 and Fig. 5:

Analysis of the above results can lead to the following conclusions:

(i) As the number of hidden layers and the number of nodes increase, the accuracy of the fitting data of the model will increase within a certain range, and the time spent on training the network also increases. When the model is particularly complicated, there may be problems such as over-fitting, training parameters need to be dynamically adjusted, and the fitting effect is not so good. Therefore, factors such as model complexity, training difficulty, and training time need to be considered when constructing the model.

(ii) When the network structure contains two hidden layers, the RMSE of the fitted data is relatively large, indicating that the results have large fluctuations, possibly due to changes in the type of restricted Boltzmann machine.

(iii) For the data set selected in this paper, the performance fitting model selects three hidden layer structures, and the first hidden layer selects 20 nodes, the second hidden layer selects 30 nodes, and the third hidden layer. When the 30 nodes are selected, the fitting effect of the model is better. At this time, the model has a 5-layer structure.

4.2.2 Comparison between DBN fitting method and neural network method:

The effects of modelling accuracy of the two methods are analysed under the condition of training samples with different data amounts. The data samples were set to 300, 500, 1000, 3000, 5000, 10,000, and 30,000 groups by random extraction, and the data was used to train the model. In order to reduce the error of the evaluation parameters caused by the random extraction of data, the data of the selected data amount is extracted multiple times in the experiment, and the obtained errors are averaged. In addition, in order to verify the effectiveness of the method, a BP neural network of the same structure was selected for comparison. From the previous analysis, the number of hidden layers of the model and the number of nodes in each layer have a relatively large impact on the final effect of the model. Therefore, in order to reduce the influence of the number of hidden layers and the number of nodes in each layer on the fitting effect, Use the method in the previous section to find the optimal network structure and then compare.

The other parameters of the neural network are set as shown in Table 4.

The experimental results are shown in Table 5. The three data from left to right in the table refer to MAPE (%), RMSE (%), and model runtime T (s).

From the above results, it can be seen that the fitting deviation (MAPE) and accuracy (RMSE) of the two methods will be improved with the increase of the data amount; When the amount of data is small, the neural network has a slightly better fitting

Table 1 Value space and initial value of the input indicator

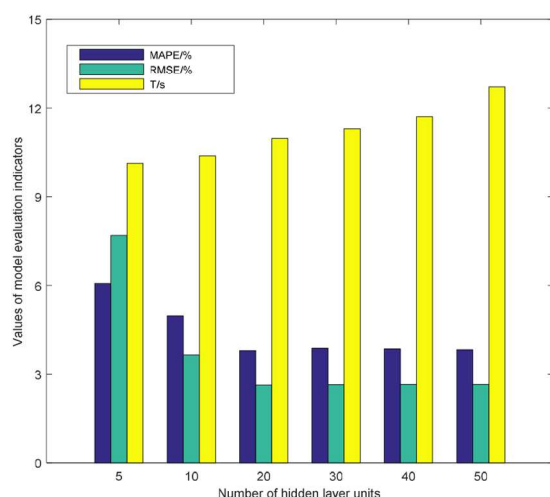
Parameter	Meaning	Value space	Initial value
x1	radar transmitting pulse power	160–200 kW	180
x2	radar antenna gain	105–115 dB	109
x3	radar working wavelength	15–30 cm	24
x4	effective scattering cross-sectional area of the target	0.1–0.5	0.3
x5	radar loss factor	16–26 dB	22
x6	radar receiver noise figure	3–8 dB	6
x7	accumulation efficiency	15–20	18
x8	weather constant	0.8–1	0.9
x9	radar maximum detection distance	150–350 km	250
x10	radar minimum detection distance	5–30 km	20
x11	the time from discovering the enemy's situation to the command receives the information	10–30 s	40
x12	the time from receiving the information to complete the preparation	10–90 s	50
x13	the time from the force receive the task to the task is completed	30–90 s	60
x14	missile damage radius	50–100 m	70
x15	missile shooting error	10–50 m	30
x16	number of missile shots	1–3	1

Table 2 Performance analysis fitting model other parameter settings

Parameter	Value
input dimension of GRBM	16
learning rate of GRNM/BRBM	0.01/0.1
the variance of GRBM	0.01
initialisation weight/offset of GRBM and BRBM	0.01
	Vecto 0.1r* randn(numvis,numhid)/Vector 0
maximum number of iterations in the pre-training and tuning phase	1000
tuning stage error function target value	0.0001

Table 3 Values of model evaluation indicators under different parameters

Number of hidden layers	Number of hidden layer units	MAPE, %	RMSE, %	Time, s
1 (GRBM)	5	6.066	7.692	10.13
	10	4.977	3.651	10.38
	20	3.796	2.636	10.97
	30	3.878	2.645	11.30
	40	3.851	2.656	11.71
2 (1GRBM, 1BRBM)	5	3.824	2.658	12.72
	5	4.858	2.265	25.97
	10	3.727	3.670	26.17
	20	2.953	2.618	26.84
	30	2.207	3.587	27.75
3 (1GRBM, 2BRBM)	40	2.208	3.581	28.64
	50	2.217	2.588	29.65
	5	2.391	2.786	34.19
	10	1.923	2.061	34.55
	20	1.519	1.988	35.50
	30	1.117	1.260	36.99
	40	1.366	1.436	36.89
	50	1.381	1.457	37.71

**Fig. 5** Effect of different node numbers on the system fitting effect when the hidden layer is 1

result; when the amount of data increases, the deviation of the fitting results (MAPE) is relatively close, and the model fitting accuracy (RMSE) proposed in this paper is better. The result has higher stability; When the amount of data is large, the proposed fitting bias (MAPE) and accuracy (RMSE) of the model are better. The model proposed in this paper takes longer than the neural network fitting method. However, since the real-time requirements are not high when using existing data for combat system optimisation, it is acceptable to use a longer time.

5 Conclusion

Reasonable performance analysis methods can effectively improve the effectiveness of warship formation air defence operations. This paper proposes a performance analysis fitting model based on DBN, which effectively reconstructs the combat model and improves the effectiveness of the effectiveness analysis results of the combat system. Firstly, the ship formation air defence

Table 4 Neural network parameter settings

Parameter	Value
number of hidden layers	one of 1, 2, 3, 4
number of neuron nodes	one of 5 10, 20, 30, 40, 50, 100, 200
network input/output dimension	16/1
training function	traingd
learning rate	0.1

Table 5 Comparison of DBN fitting method and neural network method

The amount of data	DBN fitting (M/R/T)	BP neural network (M/R/T)
100	6.015/5.405/1.74	4.738/3.359/0.75
300	3.514/3.056/1.95	3.487/3.598/0.74
500	2.383/1.401/2.15	2.939/2.383/0.71
1000	2.236/1.474/2.42	2.847/1.980/0.72
3000	2.013/1.151/2.68	2.740/1.589/0.71
5000	1.234/1.465/4.81	2.766/1.416/0.75
10,000	1.192/1.416/7.15	2.527/1.219/0.76
30,000	1.010/1.087/9.30	2.487/1.135/0.79

effectiveness analysis index system is constructed, and then the structure and training method of the performance analysis fitting model are introduced. Finally, based on the formation of air defence combat, the performance analysis fitting model based on DBN and its comparative experiments are simulated and analysed. The simulation results verify that the model has higher fitting accuracy under the same conditions.

6 Acknowledgments

This research was supported by The Aeronautical Science Foundation of China (no. 2017ZC53021) and The Open Project Fund of CETC Key Laboratory of Data Link Technology (no. CLDL-20182101).

7 References

- [1] Boardman, N.T., Lunday, B.J., Robbins, M.J.: 'Heterogeneous surface-to-air missile defence battery location: a game theoretic approach', *J. Heuristics*, 2017, **23**, (6), pp. 1–31
- [2] Qin, J., Wu, X.: 'Fire distribution of the ship-to-air missiles in the warship formation based on the market auction mechanism'. 36th Chinese Control Conf., Dalian, Liaoning, China, 2017, pp. 10155–10159
- [3] Ming, S., Jun-qing, H., Ya-long, M.A.: 'Research on methodology of operational efficiency evaluation based on combat simulation data', *J. Syst. Simul.*, 2013, **25**, (S1), pp. 366–371
- [4] Guo-wei, L., Fu-ming, W., Nan-xing, W.: 'Joint terrorism combat command system effectiveness evaluation based on fuzzy AHP in cyberspace', *J. Ordnance Equip. Eng.*, 2016, **37**, (4), pp. 111–113
- [5] Jie, L., Wen, G.: 'Continuum topology optimization considering uncertainties in load locations based on the cloud model', *Eng. Optim.*, 2017, **50**, (2), pp. 1041–1060
- [6] Fischer, A.: 'Training restricted Boltzmann machines', 2014, **29**, pp. 5–13
- [7] Sutskever, I., Tieleman, T.: 'On the convergence properties of contrastive divergence'. Proc. 13th Int. Conf. on Artificial Intelligence and Statistics (ICAIS), Sardinia, Italy, 2010, pp. 789–795d
- [8] Xiaohai, Z., Xinwen, C., Songtao, G., et al.: 'Research on intelligence of military auxiliary decision-making system based on deep learning', *J. Ordnance Equip. Eng.*, 2018, **39**, (10), pp. 162–167
- [9] Al-Fatlawi, A.H., Ling, S.H., Mohammed, H.: 'Jabardi diagnosis system for Parkinson's disease using speech characteristics of patients and deep belief network', *CAAI Trans. Intell. Technol.*, 2017, **02**, (9), pp. 246–253
- [10] Hinton, G.E., Osindero, S., Teh, Y.W.: 'A fast learning algorithm for deep belief nets', *Neural Comput.*, 2014, **18**, (7), pp. 1527–1554
- [11] Fischer, A., Igel, C.: 'Training restricted Boltzmann machines: an introduction', *Pattern Recognit.*, 2014, **49**, (1), pp. 25–39